

To appear in *Astrophysical Journal*, 1998 Vol. 499.

Gamma-Ray Spectral States of Galactic Black Hole Candidates

J.E. Grove¹, W.N. Johnson, R.A. Kroeger, K. McNaron-Brown², J.G. Skibo
E.O. Hulburt Center for Space Research, Code 7650, Naval Research Lab., Washington DC
20375

B.F. Phlips
Universities Space Research Association, Washington DC 20024

ABSTRACT

OSSE has observed seven transient black hole candidates: GRO J0422+32, GX339-4, GRS 1716-249, GRS 1009-45, 4U 1543-47, GRO J1655-40, and GRS 1915+105. Two gamma-ray spectral states are evident and, based on a limited number of contemporaneous X-ray and gamma-ray observations, these states appear to be correlated with X-ray states. The former three objects show hard spectra below 100 keV (photon number indices $\Gamma < 2$) that are exponentially cut off with folding energy ~ 100 keV, a spectral form that is consistent with thermal Comptonization. This “breaking gamma-ray state” is the high-energy extension of the X-ray low, hard state. In this state, the majority of the luminosity is above the X-ray band, carried by photons of energy ~ 100 keV. The latter four objects exhibit a “power-law gamma-ray state” with a relatively soft spectral index ($\Gamma \sim 2.5 - 3$) and no evidence for a spectral break. For GRO J1655-40, the lower limit on the break energy is 690 keV. GRS 1716-249 exhibits both spectral states, with the power-law state having significantly lower gamma-ray luminosity. The power-law gamma-ray state is associated with the presence of a strong ultrasoft X-ray excess ($kT \sim 1$ keV), the signature of the X-ray high, soft (or perhaps very high) state. The physical process responsible for the unbroken power law is not well understood, although the spectra are consistent with bulk-motion Comptonization in the convergent accretion flow.

Subject headings: Black Holes — Gamma Rays: Observations — X-rays:Binaries

¹E-mail: grove@osse.nrl.navy.mil

²CSI, George Mason University, Fairfax, VA 22030

1. Introduction

The question of whether neutron stars and black holes can be distinguished by their X-ray and gamma-ray spectra is important, and bears on the classification of newly discovered transients. Before such distinctions can be made reliably, the full range of spectral forms must be observed and categorized. Extensive knowledge of the X-ray emission of these objects has accumulated in the literature, but the nature of the gamma-ray emission is only now coming to light.

The historical record of X-ray (i.e. <30 keV) observations of galactic black hole candidates (BHCs) reveals at least four spectral states, listed here in order of decreasing X-ray luminosity (see, e.g., Tanaka 1989, Grebenev et al. 1993, and van der Klis 1994, 1995). In the “*X-ray very high*” state, the soft (i.e. 1–10 keV) X-ray flux is quite high, with an “ultrasoft” thermal or multi-color blackbody spectrum of characteristic temperature $kT \sim 1$ keV; a power-law tail is present with a photon number index $\Gamma \sim 2$ –3. The typical X-ray luminosity is approximately at the Eddington limit. Rapid intensity variations are observed and are associated with the power-law tail. The amplitude of this rapid variability is less than that in the X-ray low, hard state but significantly stronger than in the X-ray high, soft state (see below). In the “*X-ray high, soft*” state, the spectrum again shows both an ultrasoft component with $kT \sim 1$ keV and a weak power-law tail that dominates above ~ 10 keV. This state is distinguished from the X-ray very high state by its lower luminosity (typically by a factor of ~ 3 –30) and weakness or absence of rapid intensity variations. The “*X-ray low, hard*” state exhibits a single power-law spectrum with photon number index $\Gamma \sim 1.5$ –2, with a typical X-ray luminosity of $<1\%$ of Eddington. (However, we show below that in this state the majority of the luminosity is carried by photons above 30 keV). Strong rapid intensity variability is observed, with rms variations of order a few tens of percent of the total emission. The “*X-ray off*” or “*quiescent*” state exhibits very low level emission with uncertain spectral shape at a luminosity $L_X < 10^{-4}$ of Eddington.

Here we summarize the low-energy gamma-ray spectra of seven transient galactic BHCs, all low-mass X-ray binaries (LMXBs), observed with OSSE on the Compton Gamma Ray Observatory (in order of increasing right ascension: GRO J0422+32, GRS 1009–45, 4U 1543–47, GRO J1655–40, GX339–4, GRS 1716–249, and GRS 1915+105) and demonstrate the existence of two spectral states in low-energy gamma rays. We compare these spectra with those of the archetypal galactic BHC, the high-mass X-ray binary Cyg X-1. Introductory remarks covering the historical record of each of these objects are given along with the details of the OSSE observations in the subsections below.

2. Observations

The OSSE instrument on the Compton GRO consists of four nearly identical large-area NaI(Tl)–CsI(Na) phoswich detector systems (Johnson et al. 1993). It can be configured to cover the energy range from $\simeq 40$ keV to 10 MeV with good spectral resolution. Simultaneously with the spectroscopy data, count-rate samples in a number of energy bands can be collected on time scales of 4–32 ms to study rapid variability. Hard X-ray transients, including those later classified as BHCs, have been high-priority targets for OSSE throughout the Compton GRO mission. They have generally been observed as targets of opportunity in response to detection of a significant flaring event by the BATSE instrument on the Compton GRO. These target-of-opportunity pointings have lasted from less than 24 hours for GRS 1009–45 to a few weeks for GRO J0422+32, depending on the strength and duration of the outburst, as well as the flexibility of the Compton observing program. Table 1 summarizes the dates on which OSSE observed the seven gamma-ray transients discussed here.

Hard X-ray lightcurves (20–100 keV) from BATSE for each transient in this study are shown in Fig. 1. Each data point corresponds to a single day. Note that one of two different flux scales is used in each panel, depending on the intensity of the emission. The total Crab nebular and pulsar emission in this band is $\simeq 0.32$ ph cm $^{-2}$ s $^{-1}$; thus the outbursts studied here peak between about 1/3 and 1.5 Crab flux units. OSSE observing periods are indicated by shaded vertical intervals in each panel. Note also that the lightcurves end on MJD 49800.0 (1995 Mar 24.0), the last date for which BATSE flux measurements are publicly available as of this writing. For some sources, this is before the last OSSE observation included in this study, and indeed before the first OSSE observation. The lightcurves, nevertheless, serve to place the OSSE measurements in the context of the recent historical behavior of each source.

2.1. GRO J0422+32

GRO J0422+32 (XN Per 1992) was discovered in outburst by BATSE in data from 1992 August 5. The lightcurve of the outburst showed a fast rise and approximately exponential decay with $\tau \simeq 40$ days, and a secondary maximum beginning $\simeq 125$ days after the onset of the initial outburst (Harmon et al. 1994). It was observed in X-rays at various times in the outburst by ASCA (Tanaka 1993a), ROSAT (Pietsch et al. 1993), and Mir/TTM (Sunyaev et al. 1993). The X-ray spectrum in all cases was consistent with a

simple power law, with no evidence for an ultrasoft component. While the mass function of $1.2 \pm 0.04 M_{\odot}$ determined by Filippenko, Matheson, & Ho (1995) is low enough that the compact object might indeed be a neutron star, the $H\alpha$ radial velocity curve and the M stellar type of the secondary imply a mass of $3.6 M_{\odot}$ for the primary. The photometric measurements of Callanan et al. (1996) support this mass estimate and give a distance of ~ 2 kpc. It was a transient radio source, exhibiting a radio lightcurve consistent with a synchrotron bubble ejection event (Shrader et al. 1994).

OSSE observed GRO J0422+32 for 33 days spanning the interval from the peak of the outburst through the decline to approximately half maximum intensity at 100 keV. There was strong, rapid intensity variability above 50 keV (rms $\simeq 30$ –40% of the total emission) and a substantial peaked noise component in the power spectrum (Grove et al. 1994). The photon spectrum was described well by the simple, exponentially truncated power-law form in Eqn. 1. While this spectral shape was valid for each observation day, there was substantial evolution of the model parameters throughout the outburst. As the intensity at 100 keV declined, the exponential folding energy increased by about 20%, with a nearly linear anticorrelation between these parameters. The TTM and HEXE instruments on Mir-Kvant observed 1992 Aug 29 – Sep 2 and reported a hard spectrum extending well above 100 keV (Sunyaev et al. 1993; Maisack et al. 1994). To create a consistent broadband spectrum, we therefore selected OSSE data only from a four-day period surrounding this interval and fit the combined spectrum (Table 2).

2.2. GRS 1009–45

The transient GRS 1009–45 (XN Vel 1993) was discovered by GRANAT/WATCH on 1993 September 12 (Lapshov, Sazonov, & Sunyaev 1993). The lightcurve above 20 keV for the discovery outburst had a fast rise and exponential decay with $\tau \simeq 5$ days (Harmon et al. 1994). The secondary outbursts, peaking ~ 35 days and ~ 85 days after the initial outburst, had substantially longer rise and fall times (see Fig. 1). The X-ray spectrum was ultrasoft (Kaniovsky, Borozdin, & Sunyaev 1993; Tanaka 1993b; Moss 1997; Ebisawa 1997). A blue optical counterpart has been identified (Della Valle & Benetti 1993), of type late-G or early-K in a 6.86 ± 0.12 h binary orbit (Shahbaz et al. 1996). A mass function has yet to be determined. The distance is estimated to be between 1.5 and 4.5 kpc.

OSSE observed GRS 1009–45 for a single 17-hour period $\simeq 9$ days after the onset of the outburst, and $\simeq 6$ days after the peak, by which time the 20–100 keV flux had decayed to $\sim 1/3$ its maximum (Harmon et al. 1994). Despite the brevity of the pointing, OSSE clearly

detected emission above 300 keV, with a power law spectrum and no evidence for a break. ASCA data from 1993 November 11 are shown in Fig. 2 together with the OSSE spectrum. The ASCA data, which have been taken from Moss (1997), have been scaled upward by a factor of ~ 30 , corresponding to the decline in the BATSE hard X-ray flux between the OSSE and ASCA observations.

2.3. 4U 1543–47

BATSE detected 4U 1543–47 on 1992 April 18 in its third known outburst since the discovery in 1971 (Matilsky et al. 1972). The X-ray spectrum in the discovery outburst was ultrasoft. Lightcurves show a fast rise and exponential decay, and multiple secondary maxima have been observed. The e-folding time of the decline of the X-ray emission from the discovery outburst was $\tau \simeq 85$ days, while BATSE measured a much shorter $\tau \simeq 2.5$ days above 20 keV in 1992. A similar difference in soft and hard X-ray decay times was observed from GS 1124–68 (Gilfanov et al. 1991). ROSAT observed 4U 1543–47 in 1992 August and September (Greiner et al. 1993), when the source was undetectable by BATSE. The X-ray spectrum was again ultrasoft. There are no reports in the literature of rapid intensity variations. The optical counterpart is an A-type dwarf at ~ 4 kpc in an unknown binary orbit (Chevalier 1989).

OSSE observed 4U 1543–47 for a nine-day period beginning about 10 days after its detection by BATSE. The outburst peaked on April 19, and had decayed to undetectability by BATSE by the time the OSSE observation began. The OSSE data indicate that the source underwent a secondary outburst during this observation, at a flux level below BATSE’s daily sensitivity. Statistically significant emission was detected by OSSE on the first six observing days, 1992 April 28 – May 3. The spectrum was a simple power law, with emission detected to at least 200 keV. While the gamma-ray luminosity varied by a factor of ~ 3 , there was no statistically significant variation in the power-law index from day to day.

2.4. GRO J1655–40

The transient X-ray source GRO J1655–40 (XN Sco 1994) was discovered by BATSE in data from 1994 July 27. Since the discovery outburst, the emission has been episodic, showing periods of weeks of strong, relatively constant emission, then returning to

quiescence (Harmon et al. 1995). The mass function is measured to be $3.35 \pm 0.14 M_{\odot}$, and optical eclipses are observed with a 2.6-day period, suggesting that the system is viewed nearly edge-on (Bailyn et al. 1995a,b). Orosz et al. (1996) estimate the mass of the compact object to be $7 M_{\odot}$. It is a strong, transient radio source with superluminal jets (Tingay et al. 1995, Hjellming & Rupen 1995) at a distance of 3.2 kpc (McKay et al. 1994, Hjellming & Rupen 1995, Bailyn et al. 1995b). In at least three cases, the X-ray outbursts were followed within days by ejection events in the radio jets.

This source has been observed by OSSE on six occasions. Results from the first five were presented by Kroeger et al. (1996). Four observations provided strong detections of a soft power-law spectrum, while in the remaining two observations the source was undetectable by OSSE. The dates of the former are given in Table 1. A simple power-law model gives a good fit to each observation, as well as to the sum of all observations with high gamma-ray luminosity, L_{γ} . Table 2 reports the photon index for the sum of the high L_{γ} observations. The envelope of the scatter of spectral index for the individual observations is 0.4. Investigation of the spectral index on ~ 90 -minute timescales reveals a weak dependence of index with L_{γ} : higher luminosity intervals tend to have more negative spectral index (i.e. a steeper spectrum). ASCA observed GRO J1655–40 on 1995 Aug 15-16, during an outburst that unfortunately was not observed by OSSE. The BATSE instrument, with its all-sky capability, monitored this outburst in its entirety. Combined ASCA and BATSE spectra show an ultrasoft excess and a soft power-law tail ($\Gamma \simeq 2.4$) extending beyond 100 keV (Zhang et al. 1997). The ASCA data plotted in Fig. 2 have been scaled by the ratio of the average OSSE flux at 40 keV to the reported BATSE flux at 40 keV for 1995 Aug 15-16 (BATSE data are not shown in the figure). The ultrasoft excess remains apparent. During the most recent OSSE observation of GRO J1655–40 (1996 Aug-Sep), the source was also observed by the Rossi XTE, so high-quality, simultaneous, broadband spectra should soon be available.

2.5. GX339–4

The highly variable black hole candidate GX339–4 (1H 1659-48.7) exhibits all four of the X-ray states (Miyamoto et al. 1991 and references therein). Its optical counterpart (Doxsey et al. 1979) lies at a distance generally assumed to be ~ 4 kpc. It is a variable radio source (Sood & Campbell-Wilson 1994), and recent evidence suggests it may have a jet (Fender et al. 1997). In the X-ray low, hard state, rapid fluctuations with rms variations as high as 30% have been observed, as well as QPOs near ~ 0.8 Hz (Grebenev et al. 1991),

~ 0.1 Hz and ~ 0.05 Hz (Motch et al. 1983). Observations by Ginga in 1991 September established that the source was in the X-ray low, hard state. Contemporaneous OSSE observations revealed that the low-energy gamma-ray emission was strong and that the spectrum was exponentially cut off (see Fig. 2 and Table 2), from which Grabelsky et al. (1995) argued that the X-ray low, hard state corresponds to gamma-ray outburst in this object. Observations performed with GRANAT (Grebenev et al. 1993) indeed show that GX339–4 exhibits distinct hard X-ray states correlated with the X-ray behavior.

OSSE has observed GX339–4 four times. The first pointing, in 1991 September, was made as a target of opportunity in response to an outburst detected by BATSE. The second observation was performed in 1991 November as part of the scheduled viewing plan, when the source happened to have very low gamma-ray luminosity (Fig. 1). Because of the potential for confusion with diffuse continuum emission from the galactic plane, we have not included these data in our analysis. The final two observations contain proprietary data and have not been included in our analysis or in Table 1.

2.6. GRS 1716–249

The transient GRS 1716–249 (GRO J1719–24, XN Oph 1993) was discovered by GRANAT/SIGMA on 1993 September 25 (Ballet et al. 1993). Observations by ASCA (Tanaka 1993c; Moss 1997; Ebisawa 1997) and Mir-Kvant (Borozdin, Arefiev, & Sunyaev 1993) showed a hard power law spectrum, with no evidence for an ultrasoft excess. Rapid intensity variations were detected by BATSE (Harmon et al. 1993) and ASCA. A strong QPO peak was apparent, with a centroid frequency that varied from ~ 0.04 Hz to ~ 0.3 Hz through the discovery outburst (van der Hooft et al. 1996). A radio (Mirabel, Rodriguez, & Cordier 1993) and optical (Della Valle, Mirabel, & Cordier 1993) low-mass counterpart has been identified at an estimated distance of $\simeq 2.4$ kpc (Della Valle, Mirabel, & Rodriguez 1994). Interpreting optical modulations at 14.7 h as a superhump period, Masetti et al. (1996) estimated the mass of the compact object to be $> 4.9 M_{\odot}$. Hjellming et al. (1996) reported a rapidly decaying radio flare following the final outburst shown in Fig. 1. This temporal coincidence suggests a connection between the hard X-ray decline and the ejection of the relativistic electrons responsible for the radio emission, and from the similarity of this event to the emergence of a relativistic radio-synchrotron jet in GRO J1655–40 (Hjellming & Rupen 1995), Hjellming et al. suggested that a relativistic jet might have been present in GRS 1716–249 at this time. The radio data were inadequate to confirm or reject this suggestion, unfortunately.

OSSE observed GRS 1716–249 five times, with the first two observations beginning about 30 days after the onset of the discovery outburst, while the 20–100 keV flux was still within 10–15% of its maximum intensity (these observations are closely spaced in time and indistinguishable in Fig. 1). The remaining three observations were made on the trailing edge of the second outburst, between the second and third outbursts, and finally near the peak of the third outburst. The gamma-ray luminosity varied by an order of magnitude between observations. There is good evidence that both spectral states were observed. The first, second, and fifth observations, all made near the peak of outbursts, show the exponentially truncated power law form of Eqn. 1, while the third is a simple power law spectrum. The spectrum of the fourth observation can be fit with either functional form, and a statistically significant distinction cannot be drawn. The exponentially truncated spectra have been summed and are shown in the upper GRS 1716–249 spectrum in Fig. 2, while the third observation is shown in the lower spectrum. The spectral parameters in Table 2 are similarly divided. OSSE has detected spectral shape changes only in this BHC and Cyg X-1 (Phlips et al. 1996). Also plotted in Fig. 2 is the X-ray spectrum from an ASCA observation on 1993 October 5 (Moss 1997), approximately three weeks before the first OSSE observation and during the discovery outburst. No ultrasoft excess is apparent, which indicates that the source is in the X-ray low, hard state.

2.7. GRS 1915+105

The transient GRS 1915+105 (XN Aql 1992) was discovered by GRANAT/WATCH on 1992 August 15 (Castro-Tirado et al. 1992). The discovery outburst began with a slow rise to maximum intensity, and since that time its hard X-ray lightcurve has been episodic (Fig. 1). On timescales of tens to thousands of seconds, the X-ray emission is dramatically variable, showing several repeating temporal structures (Greiner, Morgan, & Remillard 1996). The X-ray spectrum is also variable: during intense flares the spectrum is cut off near 5 keV, while during more stable periods it shows an ultrasoft disk blackbody plus a power law with $\Gamma = -2.2$ (Greiner et al. 1996). At a distance of $\simeq 12.5$ kpc, it was the first object in our galaxy shown to have superluminal radio jets (Mirabel & Rodriguez 1994). As with GRO J1655–40, radio flares frequently, although not always, follow hard X-ray flares and occur during a decrease in the hard X-ray emission (Foster et al. 1996). Mirabel et al. (1997) have suggested that the companion is a high-mass late Oe or early Be star. A mass function for the system is not yet available.

OSSE observed GRS 1915+105 on three occasions, all of which are after the final day shown in Fig. 1. Extrapolating the best-fit power law model parameters from each of

these viewing periods into the 20–100 keV band gives 0.09, 0.07, and 0.07 ph cm⁻² s⁻¹, respectively, indicating that both observations were near the historical peak hard X-ray intensity for this source (compare Fig. 1). In all cases, the spectrum is a simple power law with no evidence for a break. As with GRO J1655–40, there is a weak anti-correlation of spectral hardness with L_γ (i.e. as L_γ increases, the spectrum becomes softer and the photon number index becomes more negative). GRS 1915+105 was observed in 1996 October by ASCA, Rossi XTE, Beppo SAX, and OSSE in a scheduled campaign during a continuing outburst, so simultaneous, high-quality, broadband spectra are forthcoming for this object.

2.8. Spectral Analysis

Photon number spectra from each BHC are shown in Fig. 2, along with the best-fit analytic model extrapolated to 10 keV. In most cases, the spectra are averaged over the entire OSSE dataset for which the source was detected. GRS 1716–249 appears in this figure twice, with the high-luminosity breaking spectra summed together, and the low-luminosity power-law spectra summed together, as discussed below. For clarity of the figure, the spectra have been multiplied by the arbitrary scaling factors indicated next to the source name. X-ray data are shown for GRO J0422+32, GRS 1009–45, GRO J1655–40, and GRS 1716–249.

We fit the average spectra using one of two general analytic spectral models, either a simple power law, or a power law that is exponentially truncated above a break energy:

$$f(E) = \begin{cases} A E^{-\Gamma} & E < E_b \\ A E^{-\Gamma} \exp(-(E - E_b)/E_f) & E > E_b \end{cases} \quad (1)$$

where A is the photon number flux, Γ is the photon number index, E_b is the break energy, and E_f is the exponential folding energy. Below the break energy, the exponential factor is replaced by unity, and the model simplifies to a power law. Best-fit model parameters are given in Table 2, along with the corresponding luminosities in the gamma-ray band (i.e. above 50 keV). Uncertainties in the model parameters are statistical only and reported as 68%-confidence intervals or 95%-confidence lower limits. If the simple power law is a statistically adequate fit, we report in Table 2 the photon number index from that model along with lower limits to E_b and E_f . Because of the strong correlation between these two parameters when neither is required by the data, to establish the lower limits we fixed $E_f = 2E_b$, since that relation roughly holds for GRO J0422+32.

For four sources — GRS 1009–45, 4U 1543–47, GX339–4, and GRS 1915+105 — little change in spectral parameters is observed from day to day or from observation to observation when the source is detected. Larger changes are observed for GRO J0422+32 (where E_f varies), GRO J1655–40 (where Γ varies), and GRS 1716–249 (where the spectral shape changes). In Table 2 we also report the range of statistically significant variability from day to day in one spectral parameter, E_f for the breaking spectra and Γ for the power-law spectra, along with the range of luminosities above 50 keV observed from day to day.

Two general spectral states in the gamma-ray band are apparent in Fig. 2. Three transients (GRO J0422+32, GX339–4, and GRS 1716–249) have breaking spectra. The X-ray photon number index is ~ 1.5 , and the exponential folding energy is ~ 100 keV. The remaining four transients (GRS 1009–45, 4U 1543–47, GRO J1655–40, and GRS 1915+105) show pure power law spectra, with a softer photon number index, in the range $\simeq 2.5$ –3. At low luminosity, GRS 1716–249 also appears to show a pure power law spectrum, with $\Gamma \simeq 2.5$.

The two spectral states have their peak luminosities in distinct energy ranges. Fig. 3 shows combined X-ray and OSSE gamma-ray spectra for several sources, plotted as luminosity per logarithmic energy interval. The sources shown in the breaking gamma-ray state, GRO J0422+32 and GRS 1716–249, have the bulk of their luminosity emitted near 100 keV, while for GRO J1655–40 in the power-law gamma-ray state, the ultrasoft component is dominant. We also note that the distinction between the spectral states is more apparent plotted in this manner.

We have searched for evidence of line emission at the energies suggested in previous observations of BHCs, i.e. at 170 keV from backscattered 511 keV radiation, near 480 keV as reported from SIGMA data on Nova Muscae (Goldwurm et al. 1992, Sunyaev et al. 1992), and at 511 keV. With OSSE’s very high sensitivity (roughly one order of magnitude greater than SIGMA’s at 511 keV), previously reported lines would be detected at high significance. For example, a broadened 480 keV line at 6×10^{-3} ph cm $^{-2}$ s $^{-1}$, the intensity reported from Nova Muscae, would have been detected by OSSE at $\sim 40\sigma$ in an average 24-hour period. As the SIGMA data suggest, these lines might indeed be variable, so we have searched our data on several timescales. Table 3 summarizes the results of our search, reporting 5σ upper limits daily, weekly, and on the total of all observations. (We chose this high statistical confidence level because of the large number of intervals searched.) The observations in Table 1 were divided into weeks of 7 contiguous days if possible; otherwise, if the number of contiguous observing days was less than 7, those contiguous days were defined as one “week.” No statistically significant narrow or moderately broadened line

emission is observed at any time from any of these objects.

3. Discussion

3.1. Is the Gamma-Ray State Correlated with Any Other Observable?

Having identified two distinct spectral states of gamma-ray emission from galactic black hole transients, we are led to consider whether the gamma-ray state is correlated with any other property of the transient, such as the X-ray spectral state, the gamma-ray luminosity, the lightcurve of the outburst, the presence or absence of rapid variability, or the emission in the radio band. These properties are summarized in Table 4 for each of the BHCs.

There is a strong correlation between the gamma-ray spectra shape and the existence of a strong ultrasoft X-ray spectral component. In no case is a strong ultrasoft excess reported during an outburst for which we find a breaking spectrum in the gamma-ray band, and in all cases for which the gamma-ray spectrum is a power law, a strong ultrasoft excess *is* reported in the X-ray band at some time during the outburst (other than for GRS 1716–249, for which there appears to be no contemporaneous X-ray data). We are led to identify the power law gamma-ray state with the X-ray high, soft state (or perhaps the X-ray very high state) and the breaking gamma-ray state with the X-ray low, hard state. In the former case, the bulk of the luminosity is carried off in ~ 1 keV photons from the ultrasoft component, while in the latter case, it is carried by ~ 100 keV photons (see Fig. 3). We note that Ebisawa, Titarchuk, & Chakrabarti (1996) reported from Ginga data that the photon number index of the power-law tail is always greater than 2 in the X-ray high, soft state and always less than 2 in the X-ray low, hard state. Our OSSE observations are consistent with this behavior; thus we are led to suggest that a measurement of the X-ray spectral index is adequate to indicate the presence or absence of the ultrasoft X-ray component. We caution, however, that the number of truly simultaneous X-ray and gamma-ray observations of BHCs is small, and further broadband observations, particularly with ASCA, Rossi XTE, or Beppo SAX and with OSSE, are required to study the correlation between X-ray and gamma-ray states in detail.

There is no apparent correlation between gamma-ray luminosity (above 50 keV) and the spectral state from source to source, since both the highest and lowest luminosity objects, GRS 1915+105 and 4U 1543–47 respectively, have power-law gamma-ray spectra.

However, in the case of the one source that appears to show a state change, GRS 1716–249, the power-law state occurs when L_γ is low. This is also the case for Cyg X–1 (Phlips et al. 1996). Thus it appears to be the case that, for an individual BHC, the power-law spectral state has lower L_γ than does the breaking state. How the *bolometric* luminosity changes is less certain and will require further simultaneous broadband observations.

Harmon et al. (1994) identified two types of black hole transients based on their lightcurves above 20 keV. The first type has a relatively fast rise followed by a more gradual decay, frequently with secondary maxima some weeks or months into the decline. The decay sometimes approaches an exponential form as seen in the soft X-ray band (Tanaka and Lewin 1995). The rise and decay times vary over a broad range, but are of the order of a few days and a few tens of days, respectively. We have labeled transients of this type as “FRED”, for fast rise and exponential decay, in Table 4. Harmon et al. use the label “X-ray novae.” The second type has a longer rise time (of order weeks) and multiple, recurrent outbursts of highly variable duration. Major outbursts tend to be of similar intensity, with active periods lasting for several years. We have labeled this type as “episodic” in Table 4. Harmon et al. call them the “slow risers.” No coherent, long-term periodicities in the high energy emission have been seen in either type of transient. We find that there is no correlation between the lightcurve type and the gamma-ray spectral state. The transients with FRED lightcurves clearly show both spectral states (e.g. compare GRO J0422+32 and GRO J1009–45), and the transients in the breaking state, GRO J0422+32 and GRS 1716–249, have clearly distinct lightcurves. Furthermore, Cyg X-1 and GRS 1716–249 exhibit *both* gamma-ray spectral states. Thus the mechanism that gates the accretion flow, and therefore regulates the production and evolution of outbursts, does not determine the physical process responsible for the gamma-ray emission.

Strong, rapid, aperiodic variability (i.e. on timescales of tens of seconds or less) is frequently reported in X-rays from BHCs in the X-ray low, hard state. Fractional rms variability is typically of order tens of percent of the average intensity. For recent reviews, see van der Klis (1994, 1995). We find that this is generally true in the gamma-ray band as well; see e.g. Grove et al. (1994) for GRO J0422+32 and van der Hooft et al. (1996) for GRS 1716–249, where in both sources strong, rapid variability and peaked noise are detected in the breaking gamma-ray state. The strong variability in both energy bands confirms the correspondence between the breaking gamma-ray state and the X-ray low, hard state. Recent results from RXTE (e.g. Morgan, Remillard, & Greiner 1997) indicate that the superluminal sources GRO J1655–40 and GRS 1915+105 in the X-ray high, soft state both show weaker rapid X-ray variability (of order several percent rms). While no such variability is detected in the gamma-ray band, the statistical upper limits are $\sim 5\%$ and thus reasonably consistent with the X-ray result (Crary et al. 1996, Kroeger et al. 1996).

For the superluminal sources GRO J1655–40 and GRS 1915+105, correlation between radio flaring and decreases in gamma-ray intensity has been noted elsewhere (Foster et al. 1996, Harmon et al. 1997). Yet this correlation is not entirely consistent: some radio flares are not followed by gamma-ray decreases, and perhaps more importantly, while the discovery outburst of GRO J1655–40 was characterized by multiple gamma-ray dips and flares accompanied by radio flares and knot ejections, later gamma-ray outbursts showed little or no radio variability (Tavani et al. 1996). We find that the gamma-ray spectral state of the superluminal sources remains unchanged within an outburst and from one outburst to the next, despite the presence or absence of a subsequent radio flare or ejection episode. Thus, while there certainly is a correlation between gamma-ray and radio events, the nature and details of the physical connection remain obscure.

3.2. Comparison with Cyg X-1

The archetypal binary for characterization and modeling of high-energy emission from black hole systems is Cyg X-1. The compact object has a mass in excess of $6 M_{\odot}$ (Gies & Bolton 1986), and the companion is a massive O-type supergiant in a 5.6-day binary orbit. Cyg X-1 is commonly in the X-ray low, hard state, and on occasion transitions to the X-ray high, soft state. Ling et al. (1987) enumerated three distinct levels in the 45–140 keV gamma-ray flux during the X-ray low, hard state, while Bassani et al. (1989) noted that the intensity of the hard X-ray flux might be anti-correlated with the soft X-ray flux. In the X-ray low, hard state, the source is radio-bright and relatively stable, while in the X-ray high, soft state, it is radio-quiet (Tanambaum et al. 1972, Hjellming 1973). The persistence of the radio emission along with weak modulation apparently at the binary period suggest the presence of an optically thick jet (Hjellming & Han 1995).

Recent broadband observations of Cyg X-1 reveal a bimodal spectral behavior in the gamma-ray band as well as the X-ray band (Phlips et al. 1996). At high L_{γ} , the spectrum is exponentially breaking with folding energy $\simeq 100$ keV, while at low L_{γ} , the spectrum is characterized by a power law with $\Gamma \simeq 2.3$. Thus Cyg X-1 fits neatly in the categories developed here for transient black holes. Furthermore, recent contemporaneous measurements with OSSE and Ginga or RXTE in both X-ray and gamma-ray states reveal that indeed the X-ray high, soft state is identified with the power law gamma-ray state, and the X-ray low, hard state is identified with the breaking gamma-ray state, a behavior equivalent to that shown in Fig. 3 (Gierlinski et al. 1997; Cui et al. 1997; Phlips et al. 1998, in preparation).

3.3. Emission Mechanisms

In recent years there has been considerable interest in advection-dominated accretion disk models (Narayan & Yi 1994; 1995a; 1995b; Abramowicz et al. 1995; Chen et al. 1995). In these models radiative cooling is inefficient, and the bulk of the gravitational binding energy liberated through viscous dissipation is advected across the event horizon of the black hole. Stable global solutions exist (Narayan, Kato, & Honma 1997; Chen, Abramowicz, & Lasota 1997) in which advective cooling dominates in the inner region where a hot optically thin two-temperature plasma is formed. This joins to a standard thin disk solution (Shakura & Sunyaev 1973; see also Frank, King, & Raine 1992) at large radii. The gamma ray emission is produced in the inner region through thermal Comptonization of soft photons, the bulk of which are probably supplied by the cool outer disk.

Ebisawa, Titarchuk, & Chakrabarti (1996) propose that the two distinct spectral indices in the hard X-ray band, corresponding to the X-ray high, soft and X-ray low, hard states, are the result of two distinct Comptonization mechanisms. In the low, hard state, the hard X-ray and gamma-ray emission is produced by thermal Comptonization of soft photons from the accretion disk. By contrast, in the high, soft state, the high-energy emission arises from bulk-motion Comptonization in the convergent accretion flow from the inner edge of the accretion disk. We find that the broadband X-ray and gamma-ray spectra in the X-ray high, soft and low, hard states are consistent with this picture. The spectra shown in Fig. 2 suggest the general scenario in which the presence of copious soft photons from the disk in the high, soft state serves to cool the electrons efficiently in the inner advection-dominated Comptonization region. In this case, Comptonization due to bulk motion dominates over that due to thermal motion. In contrast, in the low, hard state, there are fewer soft photons, hence higher temperatures in the Comptonization region (i.e. $\sim 50\text{--}100$ keV, rather than ~ 1 keV), and thermal Comptonization dominates.

We note that Ebisawa et al. (1996) predict that the power law spectrum from bulk-motion Comptonization will be sharply cut off near the electron rest mass-energy, $m_e c^2$, somewhere in the 200–500 keV band, because the efficiency of Comptonization drops due to increasing electron recoil as the photon energy increases. However, a recalculation by Titarchuk, Mastichiadis, & Kylafis (1996), including the term dependent on the second order in the velocity of the bulk flow, shows that the cutoff energy is substantially increased, to beyond $m_e c^2$, without affecting the power-law index. Thus the extended power-law spectrum from GRO J1655–40 does indeed appear to be consistent with bulk-motion Comptonization.

Recently Narayan, Garcia, & McClintock (1997) have compared the long-term X-ray

luminosity variations of neutron star and black hole X-ray transients and have found that the black hole transients display much larger luminosity variations between quiescence and outburst than do neutron stars. They attributed this to the fact that black holes have horizons, whereas neutron stars have material surfaces. Their study is based upon the luminosities measured in the 0.5–10 keV band using sources in outburst in both the X-ray low, hard state (e.g. V404 Cyg) and the X-ray high, soft state (e.g. A0620–00). It is evident from Fig. 3 that in fact the total luminosity in the X-ray low, hard state is substantially higher than the 0.5–10 keV luminosity, and therefore that the true variation between quiescence and outburst in these sources is likely to be substantially greater than Narayan et al. estimate. Indeed the spectra in Fig. 3 indicate that the luminosity above 50 keV (10 keV) exceeds that in the 0.5–10 keV band by a factor of $\simeq 4$ ($\simeq 6$). Unfortunately, no gamma-ray detections of BHCs in the quiescent state exist at this date, and therefore true measurements of the variation in bolometric luminosity cannot yet be made.

The observations we report here of transients in the X-ray low, hard state are entirely consistent with high-energy emission from thermal Comptonization. The spectra smoothly turn over with e-folding energy $E_f \sim 100$ keV, which implies an electron temperature of $kT \lesssim 100$ keV for the Comptonizing plasma. The spectral indices of the power law portion are $\Gamma \simeq 1.5$, which at temperatures ~ 100 keV imply Thompson depths $\tau_T \gtrsim 1$ for scattering in a spherical plasma cloud (Skibo et al. 1995).

As is the case for Cyg X-1 (Gierlinski et al. 1997), the source GRO J0422+32 appears to be “photon starved” in that the gamma ray luminosity greatly exceeds the soft X-ray luminosity. This starvation and, in the case of GRO J0422+32, the apparent absence of a reflection component argue against the disk-corona geometry (Haardt & Maraschi 1993), but are consistent with a geometry where the Comptonizing region forms a quasi-spherical cloud near the black hole as predicted by advection-dominated models.

4. Conclusions

We have demonstrated the existence of two distinct spectral states of gamma-ray emission from galactic BHCs. The first state exhibits a relatively hard power-law component with photon index roughly 1.5 that breaks at $\simeq 50$ keV and is exponentially truncated with an e-folding energy of $\simeq 100$ keV. This “breaking gamma-ray” is firmly identified with the X-ray low, hard state, i.e. with the absence or weakness of an ultrasoft X-ray component. Sources exhibiting this spectral signature include GRO J0422+32 and GRS 1716–249, as well as GX 339–4 and Cyg X-1 in their X-ray low, hard states. The second state exhibits

a relatively soft power-law gamma-ray spectrum with photon index roughly 2–3 and no evidence of a break. In the case of GRO J1655–40, the lower limit on the break energy is 690 keV, above the electron rest mass. This “power law gamma-ray” state is identified with the presence of an ultrasoft X-ray component, which is the signature of the X-ray high, soft state and the X-ray very high state. Because of the paucity of simultaneous X-ray and gamma-ray observations and the difficulty of distinguishing between the two X-ray high states, the identification of the power law gamma-ray state with which of the two high states is somewhat uncertain, although Cyg X-1 observations indicate that the correspondence is with the high, soft state (Cui et al. 1997). Sources exhibiting the power law gamma-ray state include GRS 1009-45, 4U 1543–47, GRO J1655–40, and GRS 1915+105, as well as Cyg X-1 in its X-ray high, soft state. Gamma-ray spectral state changes have now been observed in GRS 1716–249 and Cyg X-1. Further simultaneous X-ray and gamma-ray spectroscopy measurements of galactic BHCs will help elucidate the details of the relationship of the emission in the two bands.

This work was supported by NASA contract S-10987-C.

Object	Observation Dates
GRO J0422+32	1992 Aug 11–27, 1992 Sep 1–17
GRS 1009-45	1993 Sep 21–22
4U 1543–47	1992 Apr 28 – May 7
GRO J1655–40	1994 Aug 4–9, 1994 Dec 7–13, 1995 Mar 29 – Apr 4, 1996 Aug 27 – Sep 6
GX 339–4	1991 Sep 5–12
GRS 1716–249	1993 Oct 25–27 ^a , 1993 Oct 30–31 ^a , 1994 Nov 9–15 ^b , 1994 Nov 29 – Dec 7 ^c 1995 Feb 1–14 ^a
GRS 1915+105	1995 Nov 21 – Dec 7, 1996 Oct 15 – 29, 1997 May 14–20

Table 1: OSSE observation list

^aBreaking gamma-ray state.

^bPower-law gamma-ray state.

^cSpectral state uncertain; data not used.

Object	$\langle \Gamma \rangle$	$\Delta\Gamma$	$\langle E_{break} \rangle$ (keV)	$\langle E_{fold} \rangle$ (keV)	ΔE_{fold} (keV)	$\langle L_\gamma \rangle$ ($\times 10^{36}$ erg/s)	ΔL_γ ($\times 10^{36}$ erg/s)
<i>Breaking gamma-ray state</i>							
GRO J0422+32	1.49 ± 0.01^a		60 ± 3^a	132 ± 2^a	120–155	19.	14.–26.
GX339–4	1.38 ± 0.08		< 50	87 ± 6	80–90	5.4	8.7–9.3
GRS 1716–249	1.53 ± 0.06		< 50	115 ± 8	80–140	6.0	2.3–11.2
<i>Power-law gamma-ray state</i>							
GRS 1009–45	2.40 ± 0.06	$\simeq 2.4$	> 160	> 320		3.9	$\simeq 3.9$
4U 1543–47	2.78 ± 0.05	$\simeq 2.8$	> 200	> 400		0.8	0.5–1.7
GRO J1655–40	2.76 ± 0.01	2.6–3.0	> 690	> 1380		6.1	5.1–9.5
GRS 1716–249	2.42 ± 0.08	$\simeq 2.4$	> 250	> 500		1.1	0.6–1.7
GRS 1915+105	3.08 ± 0.06	2.9–3.3	> 390	> 780		31.	27.–45.

Table 2: Best-fit model parameters

^aOSSE data from 1992 Aug 26–27 and Sep 1–2 only.

Note. — Fits are performed over sum of entire data set for each object for which there was detectable emission, except for GRO J0422+32, where the fit is for the contemporaneous HEXE and OSSE observation, and for GRS 1716–249, where the fit is performed separately for the sum of observations in each spectral state (see text). Errors are 68% confidence. Lower limits on exponential folding energies are 95% confidence. Upper limits on break energies are set at OSSE threshold for spectroscopy. Luminosity is for energies above 50 keV. Ranges for spectral index, folding energy, and luminosity from daily fits are given in the columns labeled by $\Delta\Gamma$, ΔE_{fold} , and ΔL_γ .

Source	Line	FWHM (keV)	Flux ($\times 10^{-4}$ ph cm $^{-2}$ s $^{-1}$) ^a		
	Centroid (keV)		Daily	Weekly ^b	Total
GRO J0422+32	170	3	<6.3	<2.3	<1.1
	170	35	<9.3	<3.5	<1.6
	480	25	<7.5	<2.8	<1.2
	511	3	<7.2	<2.7	<1.2
GRS 1009–45	170	3	<6.3	<4.5	<4.5
	170	35	<8.9	<6.5	<6.5
	480	25	<7.8	<5.8	<5.8
	511	3	<7.7	<5.7	<5.7
4U 1543–47	170	3	<5.4	<1.7	<1.7
	170	35	<7.6	<2.4	<2.4
	480	25	<7.1	<2.3	<2.3
	511	3	<6.8	<2.3	<2.3
GRO J1655–40	170	3	<5.1	<2.2	<0.9
	170	35	<7.2	<3.1	<1.3
	480	25	<6.2	<2.6	<1.1
	511	3	<6.1	<2.6	<1.0
GX 339–4	170	3	<5.7	<2.0	<1.3
	170	35	<8.7	<3.1	<1.9
	480	25	<6.1	<2.3	<1.4
	511	3	<6.1	<2.2	<1.3
GRS 1716–249	170	3	<10.2	<4.0	<2.1
	170	35	<15.0	<5.9	<3.1
	480	25	<11.5	<5.0	<2.6
	511	3	<10.3	<4.6	<2.4
GRS 1915+105	170	3	<5.8	<2.0	<1.2
	170	35	<7.9	<2.8	<1.6
	480	25	<6.9	<2.4	<1.4
	511	3	<6.8	<2.4	<1.8

Table 3: Upper limits on narrow and broad line emission

^aUpper limits are 5σ ($\Delta\chi^2 = 25$).

^bDenotes an interval of one to ten contiguous days, depending on the source (see text).

Object	Ultrasoft Component?	L_γ (>50 keV) ($\times 10^{36}$ erg/s)	Lightcurve Type	Timing Noise?		Radio Emission?
				<20 keV	>50 keV	
<i>Breaking gamma-ray state</i>						
GRO J0422+32	No ^a	14.–26.	FRED	?	Strong	Transient ^b
GX339–4	No ^c	8.7–9.3	Episodic	Strong ^c	Weak	Variable; jet? ^d
GRS 1716–249	No ^e	2.3–11.2	Episodic	Strong ^f	Strong	Transient; jet? ^g
<i>Power-law gamma-ray state</i>						
GRS 1009–45	Yes ^h	$\simeq 3.9$	FRED	Weak ^f	UL	?
4U 1543–47	Yes ⁱ	0.5–1.7	FRED	?	UL	?
GRO J1655–40	Yes ^j	5.1–9.5	Episodic	Moderate ^k	UL	SL jet ^l
GRS 1716–249	?	0.6–1.7	Episodic	?	UL	Jet? ^g
GRS 1915+105	Yes ^m	27.–45.	Episodic	Moderate ^k	UL	SL jet ⁿ

Table 4: Phenomenological summary of black-hole transients.

References. — (a) Tanaka 1993a; (b) Shrader et al. 1994; (c) Miyamoto et al. 1991; (d) Sood & Campbell-Wilson 1994; Fender et al. 1997; (e) Tanaka 1993c; Borozdin, Arefiev, & Sunyaev 1993; (f) Ebisawa 1997; (g) Hjellming & Rupen 1995; Hjellming et al. 1996; (h) Kaniorsky, Borozdin, & Sunyaev 1993; Tanaka 1993b; (i) Matilsky et al. 1972; Greiner et al. 1993; (j) Zhang et al. 1997; (k) Morgan, Remillard, & Greiner 1997; (l) Tingay et al. 1995; Hjellming & Rupen 1995; (m) Greiner et al. 1996; (n) Mirabel & Rodriguez 1994.

Note. — “FRED” denotes a fast rise and exponential decay lightcurve. The symbol “?” indicates no reports in the literature. “UL” indicates no evidence at the sensitivity of the OSSE observations; only an upper limit is available. “SL jet” indicates apparent superluminal radio jet.

REFERENCES

- Abramowicz, M. A., Chen, X., Kato, S., Lasota, J.-P., & Regev, O. 1995, *ApJ*, 438, L37
- Bailyn, C. D. et al. 1995a, *Nature*, 374, 701
- Bailyn, C. D. et al. 1995b, *IAU Circ.* 6173
- Ballet, J. et al. 1993 *IAU Circ.* 5874
- Bassani, L, et al. 1989, *ApJ*, 343, 313
- Borozdin, K. Arefiev, V., & Sunyaev, R. 1993, *IAU Circ.* 5878
- Callanan, P. J. et al. 1996, *ApJ*, 461, 351
- Castro-Tirado, A. et al. 1992, *IAU Circ.* 5590
- Chen, X., Abramowicz, M. A., Lasota, J.-P., Narayan, R., & Yi, I. 1995, *ApJ*, 443, L61
- Chen, X., Abramowicz, M. A., & Lasota, J.-P. 1997, *ApJ*, 476, 61
- Chevalier, C., 1989, *Proc. 23rd ESLAB Symp.*, ESA SP-296, p. 341
- Crary, D. J. et al. 1996, *ApJ*, 463, L79
- Cui, W. et al. 1997, *ApJ*, 474, L57
- Della Valle, M., Mirabel, F. & Cordier, B. 1993, *IAU Circ.* 5876
- Della Valle, M. & Benetti, S. 1993, *IAU Circ.* 5890
- Della Valle, M., Mirabel, I. F. & Rodriguez, B. F. 1994, *A&A*, 290, 803
- Dermer, C. D. & Gehrels, N. 1995, *ApJ*, 447, 103
- Doxsey, R. et al. 1979, *ApJ*, 228, L67
- Ebisawa, K., Titarchuk, L., & Chakrabarti, S.K. 1996, *PASJ*, 48, 59
- Ebisawa, K. 1997, in *All Sky X-ray Observations in the Next Decade*, in press
- Fender, R. P. et al. 1997, *MNRAS*, 286, 629
- Filippenko, A. V., Matheson, T., & Ho, L. C. 1995, *ApJ*, 460, 932
- Foster, R. S. et al. 1996, *ApJ*, 467, L81
- Frank, J., King, A. R., & Raine, D. 1992, *Accretion Power in Astrophysics* (Cambridge: Cambridge University Press)
- Gierlinkski, M. et al. 1997, *MNRAS*, in press
- Gies, D.R. & Bolton, C.T. 1986, *ApJ*, 304, 371
- Gilfanov, M. et al. 1991, *Sov. Astron. Lett.*, 17, 437

- Goldwurm, A. et al. 1992, ApJ, 389, L79
- Grabelsky, D.A. et al. 1995, ApJ, 441, 800
- Grebenev, S. A. et al. 1991, Sov. Astr. Lett., 17, 413
- Grebenev, S. et al. 1993, A&AS, 97, 281
- Greiner, J. et al. 1993, in The Second Compton Symposium, eds. C.E. Fichtel, N. Gehrels, & J.P. Norris, (AIP, New York), p. 314
- Greiner, J., Morgan, E. H., & Remillard, R. A. 1996, 473, L107
- Grove, J. E. et al. 1994 in The Second Compton Symposium, eds. C.E. Fichtel, N. Gehrels, & J.P. Norris, (AIP, New York), p. 192
- Haardt, F. & Maraschi, L. 1993, ApJ, 413, 507
- Harmon, B. A. et al. 1994 in The Second Compton Symposium, eds. C.E. Fichtel, N. Gehrels, & J.P. Norris, (AIP, New York), p. 210
- Harmon, B. A. et al. 1995, Nature, 374, 703
- Harmon, B. A. et al. 1997, ApJ, 477, L85
- Hjellming, R. M. 1973, ApJ, 182, L29
- Hjellming, R. M. & Rupen, M. P., 1995, Nature, 375, 464
- Hjellming, R. M. et al. 1996, ApJ, 470, L105
- Hjellming, R. M. & Han, X. 1995, in *X-Ray Binaries*, eds. W.H.G. Lewin, J. van Paradijs, & E.P.J. van den Heuvel, p. 308
- Johnson, W.N. et al. 1993, ApJS, 86, 693
- Kaniovsky, A., Borozdin, K., & Sunyaev, R. 1993, IAU Circ. 5878
- Kroeger, R. A., et al. 1996, A&AS, 120, 117
- Lapshov, I., Sazonov, S. & Sunyaev, R. 1993, IAU Circ. 5864
- Ling, J. C. & Mahoney, W. A. 1989, ApJ, 343 157
- Maisack, M. et al. 1994, in The Second Compton Symposium, eds. C.E. Fichtel, N. Gehrels, & J.P. Norris, (AIP, New York), p. 346
- Masetti, N. et al. 1996, A&A, 314, 123
- Matilsky, T. A. et al. 1972, ApJ, 174, L53
- McKay, D. et al. 1994, IAU Circ. 6062
- Mirabel, F., Rodriguez, L. F., & Cordier, B. 1993, IAU Circ. 5876

- Mirabel, I. F. & Rodriguez, L.F. 1994, *Nature*, 371, 46
- Mirabel, I. F. et al. 1997, *ApJ*, 477, L45
- Miyamoto, S. et al. 1991, *ApJ*, 383, 784
- Morgan, E. H., Remillard, R. A., & Greiner, J. 1997, *ApJ*, 482, 993
- Moss, M. J. 1997, Ph.D. Thesis, Rice University
- Motch, C. et al. 1983, *A&A*, 119, 171
- Nandra, K. & Pounds, K. A. 1994, *MNRAS*, 268, 405
- Narayan, R. & Yi, I. 1994, *ApJ*, 428, L13
- Narayan, R. & Yi, I. 1995a, *ApJ*, 444, 231
- Narayan, R. & Yi, I. 1995b, *ApJ*, 452, 710
- Narayan, R., Kato, S., & Honma, F. 1997, *ApJ*, 476, 49
- Narayan, R., Garcia, M. R., & McClintock, J. E. 1997, *ApJ*, 478, L79
- Orosz, J. A. et al. 1996, *ApJ*, 468, 380
- Phlips, B.F. et al. 1996, *ApJ*, 465, 907
- Phlips, B.F. et al. 1997, *ApJ*, in preparation
- Pietsch N. et al. 1993, *A&A*, 273, L11
- Shahbaz, T. et al. 1996, *MNRAS*, 282, L47
- Shakura, N. I. & Sunyaev, R. A. 1973, *A&A*, 24, 337
- Shrader, C. et al. 1994, *ApJ*, 434, 698
- Skibo, J. G., Dermer, C. D., Ramaty, R., & McKinley, J. M. 1995, *ApJ*, 446, 86
- Sood, R. & Campbell-Wilson, D. 1994, *IAU Circ.* 6006
- Sunyaev, R. A. et al. 1992, *A&A*, 280, L1
- Sunyaev, R. et al. 1993, *ApJ*, 389, L75
- Tanaka, Y. 1989, in *Proc. 23rd ESLAB Symp. on Two Topics in X-Ray Astronomy* (Bologna), ESA SP-296, 3
- Tanaka Y. 1993a, *IAU Circ.* 5851
- Tanaka Y. 1993b, *IAU Circ.* 5888
- Tanaka Y. 1993c, *IAU Circ.* 5877
- Tanaka, Y. and Lewin, W. 1995, in *X-ray Binaries* (W. Lewin, J. v. Paradijs and E. v.d. Heuvel, eds.), Cambridge Univ. Press, p. 126

- Tananbaum, H. et al. 1972, ApJ, 177, L5
- Tavani, M. et al. 1996, ApJ, 473, L103
- Tingay, S. J. et al. 1995, Nature, 374, 141
- Titarchuk, L., Mastichiadis, A., & Kylafis, N.D., 1996, A&AS, 120, 171
- van der Hooft, F. et al. 1996, ApJ, 458, L75
- van der Klis, M. 1994, ApJS, 92, 511
- van der Klis, M. 1995, in *X-ray Binaries* (W. Lewin, J. v. Paradijs and E. v.d. Heuvel, eds.), Cambridge Press, p. 252
- von Montigny, C. et al. 1995, ApJ, 440, 925
- Zdziarski, A. A., Gierlinski, M., Gondek, D., & Magdziarz, P. 1997, A&A, 120, 553
- Zhang, S.N. et al. 1997, ApJ, 479, 381

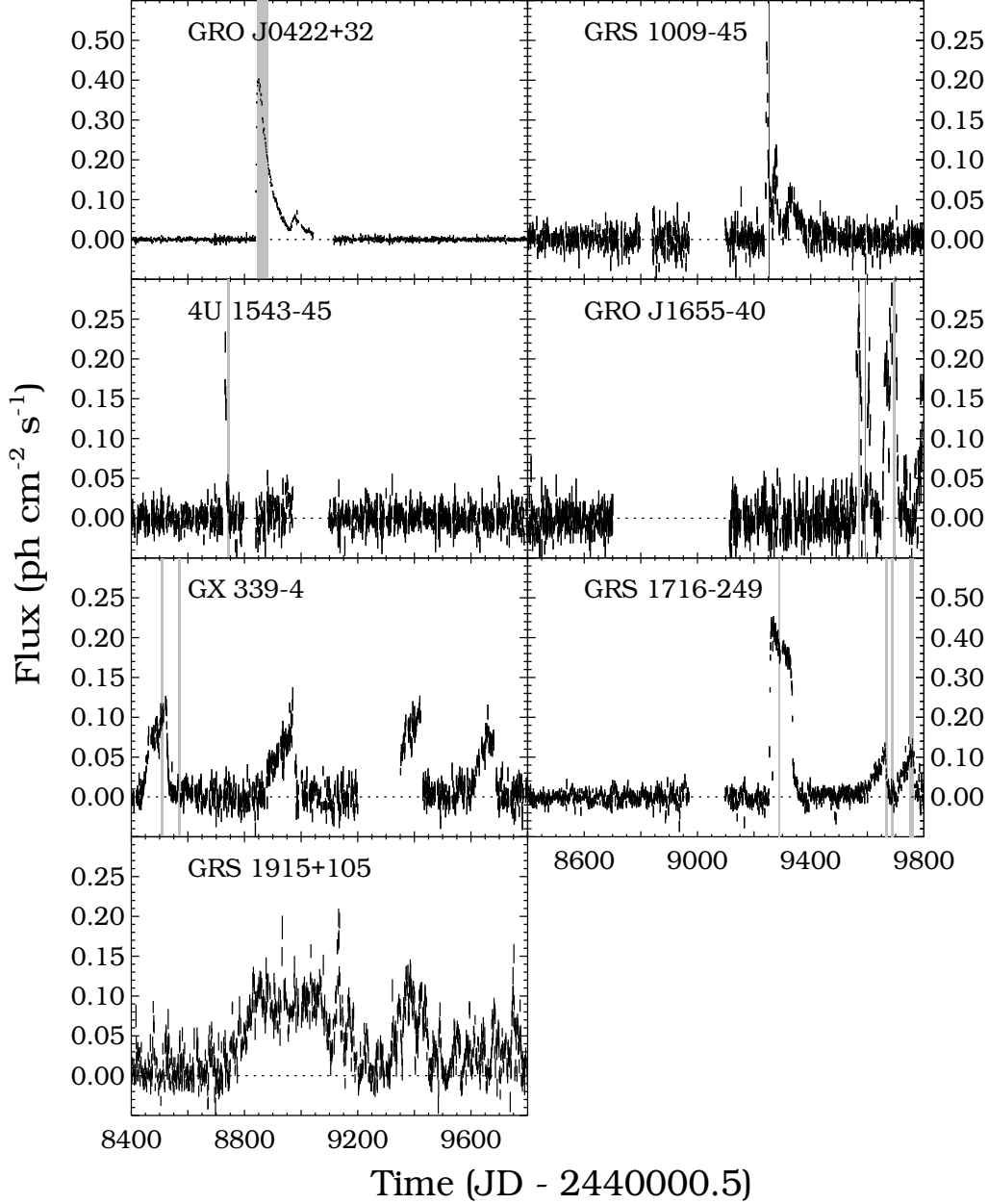


Fig. 1.— Lightcurves for seven transient BHCs in the 20–100 keV band as measured by BATSE. Each data point corresponds to a single day (JD 2448400.5 is 1991 May 24.0). The total Crab emission in this band is $\simeq 0.32 \text{ ph cm}^{-2} \text{ s}^{-1}$. Days on which OSSE observed each source are indicated by shaded regions. Note that some OSSE observations occurred following the time period covered in each panel (e.g. all observations of GRS 1915+105).

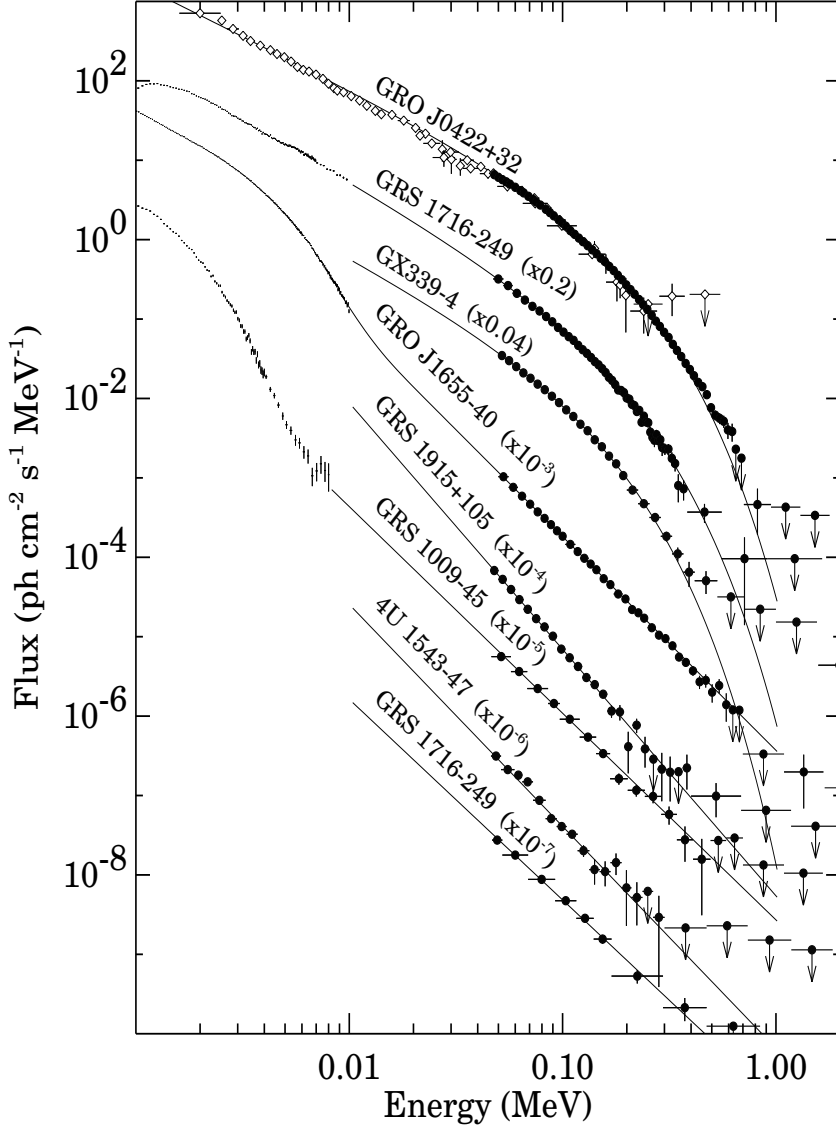


Fig. 2.— Photon number spectra from OSSE for seven transient BHCs. Spectra are averaged over all observing days for which there was detectable emission and, for clarity of the figure, have been scaled by arbitrary factors. Two spectral states are apparent. Contemporaneous TTM and HEXE data (open diamonds) and ASCA data (crosses) are shown for GRO J0422+32 and GRS 1716–249, respectively. Non-contemporaneous ASCA data (crosses) are shown for GRS 1009–45 and GRO J1655–40, scaled as indicated in the text.

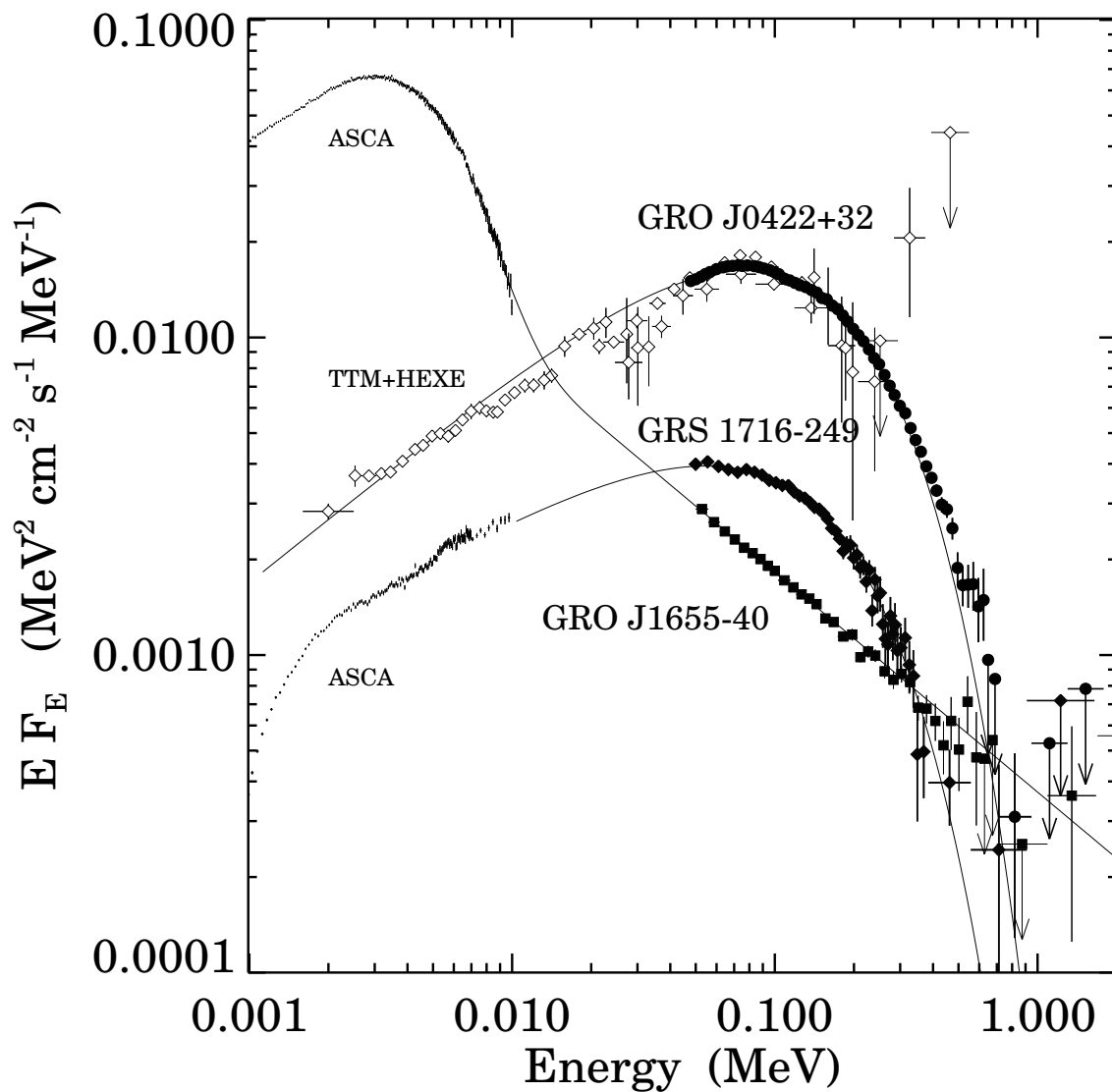


Fig. 3.— Luminosity per logarithmic energy interval for those transient BHCs with best-quality broadband spectral data. Contemporaneous TTM and HEXE data (open diamonds) and ASCA data (crosses) are shown for GRO J0422+32 and GRS 1716–249, respectively. Non-contemporaneous ASCA data are shown for GRO J1655–40 (crosses), scaled as indicated in the text.